CrystEngComm

Accepted Manuscript

ROYAL SOCIETY OF CHEMISTRY

www.rsc.org/crystengcomm

CrystEngComm

RSCPublishing

ARTICLE

Effect of fatty acid on the formation of ITO nanocrystals *via* one-pot pyrolysis reaction

Cite this: DOI: 10.1039/xoxxoooooox

Shaojuan Luo,[a] Jiyun Feng [a] and Ka Ming Ng[a*]

Received ooth January 2012,
Accepted ooth January 2012

DOI: 10.1039/xoxxoooooox

www.rsc.org/

Indium-tin carboxylate precursors were successfully synthesized by a direct reaction of indium and tin metals with a molten fatty acid under a nitrogen atmosphere at 260 °C. A linear relationship between the reaction initiation temperature and the number of carbon atoms of the fatty acids ranging from capric acid to stearic acid was observed. There was a 7 °C increase in the reaction initiation temperature for an increase of one carbon atom in the fatty acid. Nearly monodisperse 7-9 nm ITO nanocrystals without agglomeration were synthesized by direct pyrolysis of the as-synthesized precursors without using additional organic solvents. The fatty acid had minor effect on the decomposition temperature and the mean ITO particle size, but affected the particle size distribution. TOF-SIMS data confirmed that the residue fatty acids on the surface of the indium tin oxide (ITO) nanoparticles served as a built-in surfactant leading to excellent dispersity of the ITO nanocrystals in non-polar solvents.

1 Introduction

In the past decade, transparent conductive materials have received a great deal of interest in the research community because of the increase in the number of electronic devices such as flat-panel displays, touch screens, solar cells, smart windows, electronic papers, TFTs and so on.[1] Transparent conductive oxides (TCO) with their transparency, electrical conductivity and UV/IR blocking properties are the dominant materials in industrial applications.

Indium tin oxide (ITO), because of its high transmittance for visible light and low electrical resistivity among TCO materials, holds over 90% of the transparent conductive material market.[2] Normally, ITO thin films are formed by sputtering. However, gas-phase deposition methods are not suitable for flexible or heat sensitive substrates (e.g., plastics and paper). Therefore, a solution deposition route should be an attractive alternative for film formation.[3] The development of TCO nanocrystals that disperse well in a solvent along with the corresponding printing technique may lead to a low cost printable transparent electrode.[4]

The thermolysis approach has been used to produce monodisperse metal oxide nanocrystals,[5-7] and ITO nanocrystals with narrow particle size distribution have been synthesized.[8-12] However, this method consumes a large amount of high boiling point organic solvents such as 1-octadecenc. Another issue is the cost and availability of the organo-metallic precursors. Hence, an efficient, low-cost method for the synthesis of ITO nanocrystals with controllable particle size and particle size distribution has both academic significance and practical industrial applications.

Our group has developed an efficient and economical method for preparing metal oxide particles. Metal oxide particles could be synthesized by pyrolyzing the organo-metallic precursors, which are obtained by a reaction between a metal and stearic acid at elevated temperatures.[13-16] Other fatty acids are expected to react with the indium and tin metals resulting in different indium-tin carboxylate precursors.

In this paper, the effect of fatty acid carbon number on the direct reaction of indium and tin metals with molten fatty acids was studied. Also investigated were the dispersity of these ITO nanocrystals thus formed in non-polar solvents such as chloroform, toluene, and n-hexane. Five fatty acids ranging from capric acid to stearic acid were selected to investigate the effect of fatty acid carbon number on the synthesis of ITO nanocrystals. These included the effect of acidity on the reaction initiation temperature and the length of the fatty acid alkyl chain on the mean ITO particle size and the particle size distribution.

2 Experimental details

2.1 Chemicals

Raw indium metal (indium ingot, 99.995%) and tin metal (tin granules, 99.999%) were purchased from Zhuzhou Smelter Group Co., PRC; stearic acid (95%), lauric acid (97%),

decanoic acid (99%) and octanoic acid (98%, liq.) were obtained from Sigma-Aldrich Company; myristic acid (98%) and palmitic acid (99%) were from Aladdin, chloroform (99.8%) and ethanol (99.9%) were from Merck, toluene (99.7%) and n-hexane (95%) were from Mallinckrodt. All the chemicals were used as received without any further purification.

2.2 Synthesis of indium-tin carboxylate precursors

0.01 mole of indium metal (1.15 g), 0.001 mole of tin granules (0.12 g, the amount of tin depends on the Sn doping level), and 0.034 mole of fatty acid were introduced into a 50 mL condenser-equipped three-neck round-bottom flask. Then, the raw materials in the flask were heated at a rate of 10 °C/min from room temperature to 260 °C, and kept at that temperature with vigorous stirring under a continuous nitrogen flow. The nitrogen atmosphere was to prevent the fatty acid from oxidizing in air. During the reaction, the fatty acids remained in molten state and bubbles came out of the reaction solution were identified to be hydrogen. At some point, the two metals disappeared, indicating that both of them reacted with the fatty acid completely. An optically clear solution with light yellow color was formed. Subsequently, the indium-tin carboxylate precursors in waxy solid form were obtained by cooling the solution to room temperature.

2.3 Synthesis of ITO nanocrystals by pyrolysis without using any organic solvents

After indium-tin metals reacting with the fatty acid completely, the as-synthesized indium-tin carboxylate precursor in the flask was heated to 300 °C at a heating rate of 10 °C/min and was then held at 300 °C for 3 hours for the pyrolysis reaction under a nitrogen atmosphere. After that, the flask was cooled down to room temperature, and the precipitate with a blue color was found at the bottom of the flask. The precipitate was washed by hot ethanol to remove the by-products, and dried at 80 °C overnight under vacuum. Finally, the ITO nanocrystals in powder form were obtained. It should be stressed that, in the pyrolysis reaction, no high boiling point organic solvents such as ODE (1-octadecene) was used, which is significantly different from the reactions for the synthesis of nanocrystals reported elsewhere.[5-12]

2.4 Characterization

Thermo gravimetric analysis (TGA) of the indium-tin carboxylate precursor was performed on Perkin Elmer, UNIX/TGA7 from room temperature to 700 °C in a nitrogen atmosphere at a heating rate of 10 °C/min. Fourier transform infrared spectra (FT-IR) of the indium-tin carboxylate precursors were obtained by using an FT-IR spectrometer (Bio-Rad, FTS6000) in attenuated total reflection (ATR) mode. Phase identification and structural analysis of the ITO nanocrystals were conducted on a Phillips X'pert Pro x-ray diffractometer equipped with Cu Kα radiation (λ = 1.54056 Å) at a scan rate of 0.5 °/s and 2θ from 10° to 70°, operating at 40 kV and 40 mA. Electron micrographs of the ITO nanocrystals were taken using a transmission electron microscope (TEM) (JEOL-2010) with an accelerating voltage of 200 kV, equipped with a Bruker energy-dispersive X-ray spectroscope (EDXS) and selected-area electron diffraction (SAED). The TEM samples were prepared by dropping an *n*-hexane dispersion of the ITO nanocrystals onto a copper grid coated with an amorphous carbon layer, followed by drying in a vacuum desiccator. TOF-SIMS analysis of the ITO nanoparticle surface was performed on TOF SIMS V (ION-TOF GmbH), and a Cs^+ source was used.

3 Results and discussion

Octanoic acid (caprylic acid, C8, liq.), decanoic acid (capric acid, C10, sol.), dodecanoic acid (lauric acid, C12, sol.), tetradecanoic acid (myristic acid, C14, sol.), hexadecanoic acid (palmitic acid, C16, sol.) and Octadecanoic acid (stearic aicd, C18, sol.) were used to investigate the reactivity between a fatty acid and indium-tin metals. In principle, an acid with a shorter aliphatic chain would show a higher acidity. For example, the acidity of stearic acid is weaker than that of acetic acid at room temperature. At some point in time of heating up the reaction system, hydrogen bubbles started to evolve from the surface of the metal. Table 1 shows the reaction initiation temperature for different fatty acids and the indium-tin metals. It was not possible to pinpoint a single temperature for gas evolution by visual observation. The reaction initiation temperature is the mean temperature of a temperature range. It can be seen in Table 1 that the reaction initiation temperature increased gradually from C10 (capric acid) to C18 (stearic acid). Caprylic acid had a rather high initiation temperature and did not follow the trend shown by other fatty acids. This is because the boiling point of caprylic acid is 239.7 °C, which is lower than our reaction temperature of 260 °C. It was decided not to lower the reaction temperature for caprylic acid that would require a much longer reaction time. However, caprylic acid cannot react completely with the metals at the temperature of 200 °C; as a result, we discard the consideration of caprylic acid in this paper. The dependency of the initiation temperature on the number of carbon atoms of the fatty acid is shown in Fig. 1. From capric acid to stearic acid, there was a 7 °C increase in the reaction initiation temperature for an increase of one carbon atom in the fatty acid. Table 2 shows the approximate reaction time for the complete reaction of the indium-tin metals with fatty acid under the same reaction temperature of 260°C. It shows an increase in complete reaction time as fatty acid size increases and capric acid possesses the highest reaction activity.

Table 1 Initiation temperature of the fatty acid and the indium-tin metals

Fatty acid	C8	C10	C12	C14	C16	C18
Temperature (°C)	177±1.4	121±2.1	130±2.8	149±2.8	167±3.5	173±2.8

Table 2 Approximate reaction time for complete reaction of the indium-tin metals with fatty acid

Fatty acid	C8	C10	C12	C14	C16	C18

Time	---	1h	1h20min	2h	2h50min	3h

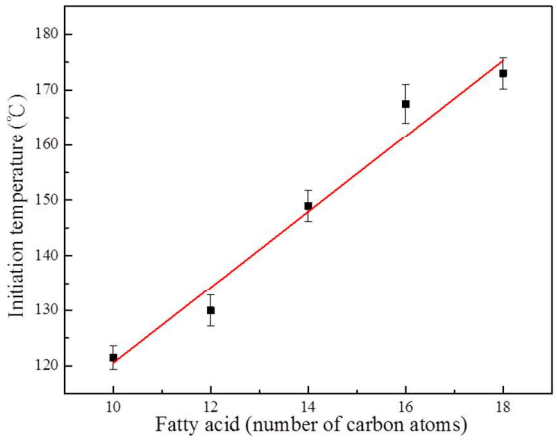

Fig. 1 The relationship between the initiation temperature and the number of carbon atoms of the fatty acid in the reaction between fatty acid and indium-tin metals.

3.1 Identification of the indium-tin carboxylate precursor

After reactions, the five solid products were characterized by FT-IR spectroscopy (ATR). As shown with arrows in Fig. 2, all five products exhibit the characteristic asymmetric COO^- stretching peaks from 1510 to 1630 cm^{-1},[12,17,18] indicating the formation of indium-tin caprate, indium-tin laurate, indium-tin myristate, indium-tin palmitate and indium-tin stearate. These results clearly confirmed the possibility of using different fatty acids to tune the properties of the indium tin oxide product.

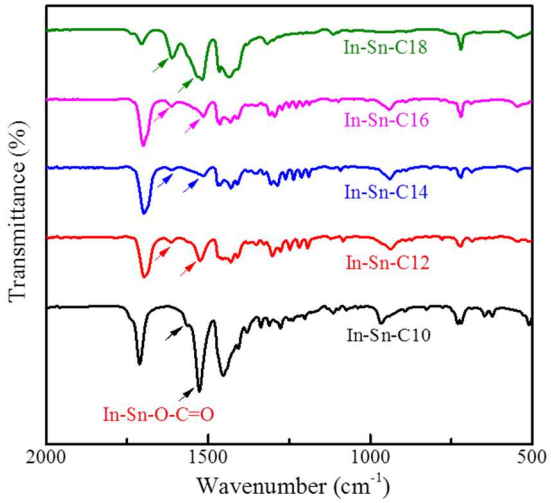

Fig. 2 FT-IR spectra of the indium-tin caprate (In-Sn-C10), indium-tin laurate (In-Sn-C12), indium-tin myristate (In-Sn-C14), indium-tin palmitate (In-Sn-C16), and indium-tin stearate (In-Sn-C18).

The as-synthesized indium-tin carboxylate precursors decomposed in a similar fashion with the main weight loss occurring in the temperature range of 300 to 375 °C (Fig. 3). The decomposition temperature occurred at a slightly higher temperature with an increase in carbon number.

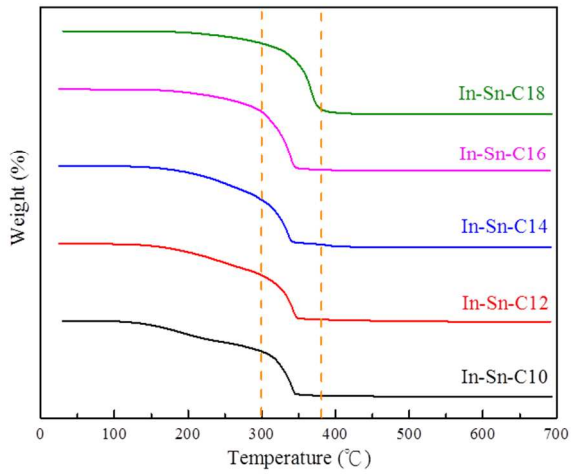

Fig. 3 TGA curves of different organo-indium-tin precursors.

3.2 Crystal structure of the ITO nanocrystals from the indium-tin carboxylate precursors

Pyrolysis of the five precursors was conducted at 300 °C under a nitrogen atmosphere for 3 hours. The blue products labelled C10-ITO, C12-ITO, C14-ITO, C16- ITO and C18-ITO were obtained in powder form. Their XRD patterns are displayed in Fig. 4. The peaks matched well the main diffraction peaks of the *bcc* indium oxide (JCPDS file No. 06-0416), and no discernible peaks of tin oxide or other indium oxide compounds were detected. The XRD results matched well with the sample C18-ITO that was prepared from indium-tin stearate.[15] The average crystallite sizes of these ITO nanocrystals were calculated from the XRD patterns using the Debye-Scherrer equation, and the results are listed in Table 3. The crystallite sizes of these ITO nanocrystals synthesized from different indium-tin carboxylate precursors were similar, ranging from 7-9 nm.

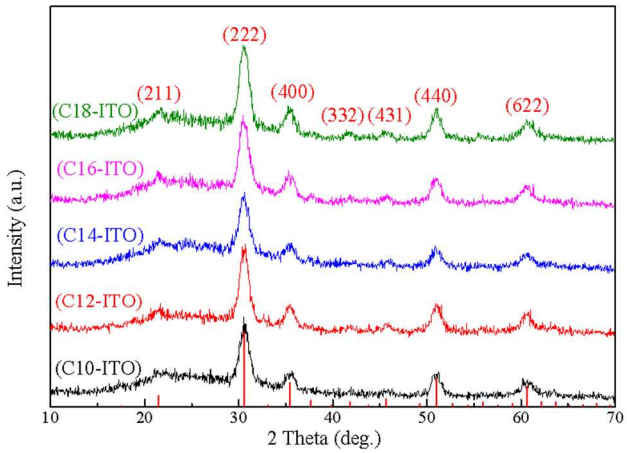

Fig. 4 XRD patterns of the ITO nanocrystals prepared by different indium-tin carboxylate precursors. The red vertical lines represent the standard patterns of *bcc* In_2O_3 (JCPDS #06-0416).

In a typical thermal decomposition process to synthesize ITO nanocrystals, indium (tin) acetate[10,12] and indium (tin) acetylacetonate[9,11] were commonly used as precursors, and

oleic acid and oleylamine as surfactants. Moreover, a high boiling point non-coordinating solvent such as 1-octadecene was often used in the reaction. While these well-established ligand protected reactions yielded high quality monodisperse nanocrystals, our precursors could achieve the same in a simpler fashion. During the reaction, the indium and tin ions dissociated from the long alkyl tail to form ITO nuclei and to grow the ITO nanocrystals. The remaining fragments of fatty acid served as surfactants to prevent the ITO nanocrystals from aggregation. Only gentle mixing was required because the indium and tin precursors were already mixed at the molecular scale.

Table 3 The calculated crystallite sizes of the as-synthesized ITO nanocrystals

Sample	C10-ITO	C12-ITO	C14-ITO	C16-ITO	C18-ITO
crystallite size (nm)	7.8	8.9	8.8	8.0	7.5

3.3 Size and morphology of the ITO nanocrystals

As mentioned, different shapes of nanocrystals can be generated by simply varying the degree of ligand protection. That is, limited ligand protection (LLP) leads to the aggregation.[17,19] Fig. 5(a)-(e) display the TEM images of five samples, one for each of the fatty acids, C10-C18. The low resolution TEM images clearly showed the nature of the nanoparticles. The mean particles size of the five samples were 6.7 nm, 7.5 nm, 7.5 nm, 7.5 nm and 7.1 nm and the corresponding relative standard deviations (RSD) were 16.0%, 16.9%, 13.8%, 11.9% and 9.8% respectively, based on sampling 300 random nanoparticles. The mean particle size results from TEM agreed well with those calculated from the XRD patterns using the Debye-Scherrer equation (Table 3). The difference of alkyl chain length seemed to have little effect on the mean particle size, but affected the particle size distribution of the ITO samples. The RSD of the particle size distribution decreases from 16.0% to 9.8% when the length of the alkyl chain increased from 10 to 18, concluding that using a longer alkyl chain fatty acid can narrow the size distribution of ITO nanocrystals.

All the as-synthesized ITO samples can be dispersed in the non-polar solvent, such as *n*-hexane, toluene and chloroform. Figure 6 shows a photo of five optically clear dispersions in chloroform. The bottles contained ITO with a concentration of 10 mg/mL prepared with the five fatty acids. The excellent dispersity of the ITO nanocrystals in non-polar solvents offers a substantial advantage for applications in solution coating and fabrication of nanocomposites.

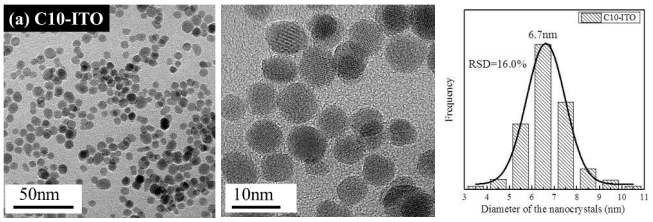

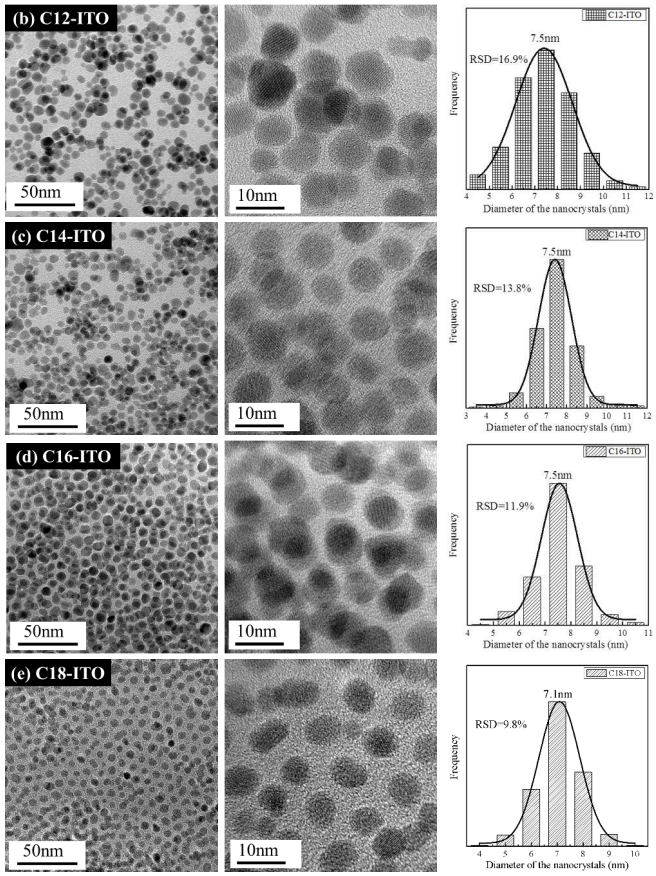

Fig. 5 Low resolution and high resolution TEM images of the (a) C10-ITO, (b) C12-ITO, (c) C14-ITO, (d) C16-ITO and (e) C18-ITO nanocrystals. The relative size distribution histograms are also shown. The curves are the corresponding Gaussian fits.

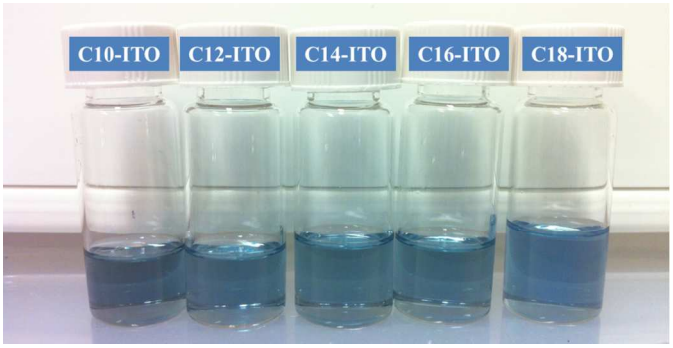

Fig. 6 A photo of ITO nanocrystal dispersions in chloroform. The concentration is 10 mg/mL.

3.4 Surface analysis of the ITO nanocrystals

The ITO nanocrystals prepared by this one-pot pyrolysis method had showed excellent dispersity. To understand the source of stability, TOF-SIMS technique was used to study their surfaces for the first time. Fig. S1 shows the TOF-SIMS negative spectra of the surfaces of the five products, which revealed fragments such as $C_{10}H_{19}O_2$ (Fig. S1a), $C_{12}H_{23}O_2$ (Fig. S1b), $C_{14}H_{27}O_2$ (Fig. S1c), $C_{16}H_{31}O_2$ (Fig. S1d) and $C_{18}H_{35}O_2$ (Fig. S1e), corresponding to the five fatty acids (C10-C18). The fragments showed two characteristics, the presence of –COOH

groups and long hydrophobic chains. The attached chemical species on the surfaces of ITO nanocrystals function as stabilizers for the ITO nanoparticles. In addition, dimer fragments $C_{30}H_{57}O_2$ and $C_{32}H_{61}O_2$ were found for palmitic acid and stearic acid. It should be also noted that the stabilizers are not single pure chemical but a mixture of different chemicals. Thus, the TOF-SIMS analysis provided solid evidence that some stabilizing entities were indeed attached to the surface of the ITO nanoparticles, forming an organic layer leading to the high dispersity of the ITO nanocrystals in non-polar solvents. Obviously, the layer was produced during the pyrolysis of the organo-metallic precursors to form ITO nanoparticles.

4 Conclusions

In summary, indium-tin carboxylate precursors were synthesized by a direct reaction between metals (indium and tin) and molten fatty acids under a nitrogen atmosphere at 260 °C for 3 hours. A linear relationship between the reaction initiation temperature and the number of carbon atoms of the fatty acid was observed. From capric acid to stearic acid, there was a 7 °C increase in the reaction initiation temperature for an increase of one carbon atom in the fatty acid. Nearly monodisperse ITO nanocrystals with an average crystallite size of 7-9 nm without agglomeration were synthesized by the direct pyrolysis of the as-synthesized precursors without using additional organic solvents. For the fatty acids considered, the alkyl chain length seemed to have little effect on the mean particle size, but affected the particle size distribution of the ITO samples. TOF-SIMS technique confirmed that the residue fatty acids formed on the surfaces of the nanoparticles during the pyrolysis reaction served as stabilizing agents. This led to excellent dispersity of the ITO nanocrystals in non-polar solvents. Although all of the five fatty acids are suitable for the formation of ITO nanocrystals, stearic acid, being the cheapest, might be a strong candidate for large-scale production

5 Acknowledgements

The authors gratefully acknowledge the financial support from the University Grants Council of the Hong Kong Government. Also, the technical support of the Raith-HKUST Nanotechnology Laboratory (project No. SEG_HKUST08) at MCPF of HKUST is also appreciated.

Notes and references

[a] *Department of Chemical and Biomolecular Engineering, The Hong Kong University of Science and Technology, Clear Water Bay, Kowloon, Hong Kong. Fax: +852 2358 0054; Tel: +852 2358 7238; E-mail: kekmng@ust.hk*
Electronic Supplementary Information (ESI) available:
See DOI: 10.1039/b000000x/

1 D.S. Ginley, H. Hosono and D.C. Paine. Handbook of transparent conductors*, New York: Springer,* 2010.
2 T.O.L. Sunde, E. Garskaite, B. Otter, H.E. Fossheim, R. Sæterli, R. Holmestad, M.A. Einarsrud and T. Grande. *J. Mater. Chen.*, 2012, **22**, 15740.
3 R.M. Pasquarelli, D.S. Ginley and R. O'hayre, etc. *Chem. Soc. Rev*, 2011, **40**, 5406.
4 E.N. Dattoli and W. Lu. *MRS Bull.*, 2011, **36**, 782.
5 J. Park, J. Joo, S.G. Kwon, Y. Jang and T. Hyeon. *Angew. Chem. Int. Ed.*, 2007, **46**, 4630.
6 J. Park, K. An, Y. Hwang, J.G. Park, H.J. Noh, J.Y. Kim, J.H. Park, N.M. Hwang and T. Hyeon. *Nat. Mater.*, 2004, **3**, 891.
7 J. Lee, S. Zhang and S. Sun. *Chem. Mater.*, 2013, **25**, 1293.
8 G. Bühler, D. Thölmann and C. Feldmann. *Adv. Mater.*, 2007, **19**, 2224.
9 S.I. Choi, K.M. Nam, B.K. Park, W.S. Seo and J.T. Park. *Chem. Mater.,* 2008, **20**, 2609.
10 Z. Sun, J. He, A. Kumbhar and J. Fang. *Langmuir*, 2010, **26**, 4246.
11 J. Lee, S. Lee, G. Li, M.A. Petruska, D.C. Paine and S. Sun. *J. Am. Chem. Soc.*, 2012, **134**, 13410.
12 R.A. Gilstrap Jr., C.J. Capozzi, C.G. Carson, R.A. Gerhardt and C.J. Summers. *Adv. Mater.*, 2008, **20**, 4163.
13 D. Yang, Y.S. Chan and K.M. Ng. U. S. non-provisional Patent application, 2014.
14 S. Luo, D. Yang, J. Zhuang and K.M. Ng. *CrystEngComm,* 2013, **15**, 8065.
15 S. Luo, D. Yang, J. Feng and K.M. Ng. *J. Nanopart. Res*., 2014, **16**, 2561.
16 S. Luo, J. Feng and K.M. Ng. *CrystEngComm*, 2014, **16**, 9236.
17 A. Narayanaswamy, H.F. Xu, N. Pradhan, M. Kim and X. Peng. *J. Am. Chem. Soc.*, 2006, **128**, 10310.
18 W. Fresenius, J.F.K. Huber, E. Pungor, G.A. Rechnitz, W. Simon and T.S. West. Tables of Spectral Data for Structure Determination of Organic Compounds, 2nd ed., *Springer-Verlag: Berlin,* 1989.
19 A. Narayanaswamy, H.F. Xu, N. Pradhan and X. Peng. *Angew. Chem. Int. Ed.*, 2006, **118**, 548.